Available online at www.sciencedirect.com

ScienceDirect

journal homepage: http://www.elsevier.com/locate/acme

Original Research Article

Microstructural characterization of cellulose fibres in reinforced cement boards

Krzysztof Schabowicz [a,*], Daria Jóźwiak-Niedźwiedzka [b], Zbigniew Ranachowski [b], Stanislav Kudela Jr. [c], Tomas Dvorak [c]

[a] Faculty of Civil Engineering, Wrocław University of Science and Technology, Wybrzeże Wyspiańskiego 27, 50-370 Wrocław, Poland

[b] Institute of Fundamental Technological Research, Polish Academy of Sciences, Pawińskiego 5B, 02-106 Warsaw, Poland

[c] Institute of Materials and Machine Mechanics, Slovak Academy of Sciences, Dúbravská Cesta 9, 845-13 Bratislava, Slovak Republic

ARTICLE INFO

Article history:
Received 22 June 2017
Accepted 27 January 2018
Available online 18 March 2018

Keywords:
Cellulose fibre reinforced cement boards
Microstructure
Fibre distribution
X-ray microtomography
SEM-EDS analysis

ABSTRACT

The microscopic analysis of the different cellulose fibre cement composites is presented. The observations of the fibres in optical microscope in transmitted light and in scanning electron microscope are described. The micro computed tomography (micro-CT) and SEM were used to determine the distribution of the fibres in the matrix. The investigated fibre cement boards were produced by extrusion process and panels were cured in natural conditions. The main goal of the research was application of different microscopic methods to analyze the fibres distribution as a result of a different methods of their production. Micro-CT was used for 3D visualization of fibres distribution in three different fibre cement boards. It was possible to determine the average diameter of the fibres and their concentration using the high-resolution mode of micro-CT scanning procedure. Finally, a procedure which can be applied as a useful tool for analysis of the different procedures used in production of fibre cement boards is described. This procedure can be successfully used in the quality control system of cellulose fibre distribution in cement composites.

1. Introduction

The use of both metallic and non-metallic fibres to improve specific properties of mortar and concrete is not new. The behaviour of concrete reinforced with different kinds of fibres, which possess good tensile strength and bond properties have been studied in detail by several investigators, e.g. [1–3]. But in recent years there has been growing interest in utilizing natural fibres. Natural fibres, such as wood and cellulose fibres, are considered environmentally sustainable materials due to their renewability and biodegradability. The relatively high

* Corresponding author.
E-mail address: k.schabowicz@pwr.edu.pl (K. Schabowicz).
https://doi.org/10.1016/j.acme.2018.01.018

cost of industrial fibres makes the use of natural fibres as possible substitutes, additionally the ecological aspect is taken into consideration to produce eco-friendly construction materials.

The cellulose fibre cement boards belong to a special class of fibre-reinforced cementitious composites. They are widely used in building construction, as siding, ceilings, floors, roofs and tile backer boards. The cellulose fibre cement siding is commonly used as a replacement for wood siding, as it is less expensive and more durable, and has lower maintenance costs [4]. The fibre cement boards also referred to as precast fabrication, are becoming more and more important in the entire construction sector. Precast of concrete in a plant offers a variety of advantages, such as efficiency of construction processes, improved quality, better budget control, consumption of less materials and less waste on site. Precast concrete products provide the builder with quicker erection times, the reduced need for plant on site, easier management of construction sites and the realization from simple to complex structures [5–7].

The final properties of cellulose fibre cement composites depend, aside from the fibre and the matrix components, on the manufacturing process. The majority of the fabrication methods for cement composites reinforced with cellulose fibres in the pulp form are based on the Hatschek process, patented by L. Hatschek in 1900. It is a semi-continuous process comprised of three steps: sheet formation, board formation, and curing [5]. Other newer methods are extrusion of pulp cement mixtures and laminates with long fibres or sheet-like structures. Extrusion allows the alignment of the pulp fibres in the machine direction and the lamination methods allow reinforcement with semi-finished products, such as unidirectional long fibres, to ensure a higher level of enforcement in the desired direction [5]. The extrusion pulping is a technically and economically viable process for the chemo-mechanical pulping of non-wood fibres. Chemo-mechanical pulping provides a much higher yield (typically 80%) and a much lower use of chemicals. Moreover, extrusion pulping also allows cutting to a desired fibre length, so subsequently the pulps can be handled by bulk papermaking systems [8].

The mechanical properties, durability and microstructure of the autoclaved Hatschek-made cellulose fibre reinforced cements in the various environments are widely described in the literature. Akhavan et al. [4] presented a procedure to manufacture fibres cement boards in the laboratory, and alternative economical methods for increasing the boards' ductility. Ductility was measured using a 3-point or 4-point bending tests, and the microstructure of the boards was studied using scanning electron microscopy. Fernández-Carrasco et al. [9] tested the vegetable-fibre cement composites free of portlandite and with short curing process, and analyzed the influence of the curing conditions and the addition of pozzolanic material on the hydration of Portland cement–fibre matrices.

The final properties of cellulose fibre cement composites and durability primarily depends on its microstructure. The information concerned the microstructure of the cellulose fibre cement boards produced by extrusion pulping process are missing. Tonoli et al. [10] analyzed the effects of natural weathering on microstructure and mineral composition of cementitious roofing tiles reinforced with fique fibre. Savastano et al. [11] tested microstructure and mechanical properties of waste fibre – cement composites, but none of them concerns the extrusion process. Soroushian et al. [12] applied the extrusion procedure to prepare cellulose pulp cement composites with up to 8 wt% fibres. He analyzed the effect of fibre origin (recycled, softwood and hardwood pulps) and content (5, 10 and 15 wt%) on cement composites processed by extrusion.

Hola, Schabowicz, et al. [13,14] presented non-destructive and semi-destructive methods of the concrete structure diagnostic in relation to their durability. They focused on the methods and techniques that are useful for assessing the durability of concrete structures depending on the main degradation mechanism and its final effects on durability. Also authors in [15–17] used acoustic methods for non-destructive identification of delaminations in cement based elements. In paper [15] an original methodology for the non-destructive identification of delaminations in concrete floor toppings using both, the impulse-response and impact-echo acoustic methods was showed. Additionally, an example of the practical use of the analyzed methodology was presented. Several non-destructive methods were compared and applied to analyze the cracked foundation slab in [16]. Berkowski et al. [17] analyzed the cracks and mechanical durability of concrete from real structure using different non-destructive methods.

Goszczynska et al. [18] used acoustic emission method for experimental validation of concrete crack identification and location. Application of acoustic emission method to determine critical stress in fibre reinforced mortar beams was presented in [19]. All of mentioned above authors made their test for concrete elements using NDT methods, only Neithalath et al. [20] presented acoustic performance and damping behaviour of cellulose-cement composites.

At the same time the X-ray microtopography technique has been developed to study the microstructures of different materials, especially for non-destructive characterization of the internal structure of porous material [21]. Li-Ping Guo et al. [22] investigated the effects of mineral admixtures on initial defects existing in high-performance concrete microstructures using a high-resolution X-ray micro-CT. Cnudde et al. [23] were using micro-CT method to determine the impregnation depth of water repellents and consolidants inside natural building stones. 3D information about the total porosity and the pore size distribution was obtained with the combination of micro-CT and home-made 3D software [24]. Wang et al. [25] used this technique to produce the X-ray tomography images of porous metal fibre sintered sheet with 80% porosity.

In general the micro-CT has been used to visualize the microstructure of concrete for some last decades. The equipment for material testing with micro-CT technique are produced at present by a few companies and these apparatus are capable to perform tests on the small specimens of few millimetres size or on large elements of a few metres. They include the microfocal source of X-ray radiation, the movable table to place a specimen, and the flat panel with a radiation detector, which resolution usually equals 2000×2000 pixels. The structure of concrete is visualized on the cross-sections (tomograms) of the investigated specimen

using grey scale convention related directly to the amount of local radiation absorption of the material. The grey scale covers several tens of grey levels and is ordered from white related to maximum of absorption to black related to the minimum, respectively. Unhydrated cement particles and aggregate grains are objects of the greatest absorption. The hydratation products that cover major part of the cement matrix present slightly lower absorption ability. The next in the line are hydrated calcinates and at the end of the scale are the organic fibres (if present) and the regions of high porosity. The image resolution of microtomograms usually varies from 1 to 10 μm per voxel (volumetric 3D pixel). The advantage of micro-CT technique is a possibility of reconstruction of 3-dimensional image of investigated objects and to determine the volumetric part of the material occupied by bulk matrix, aggregates, voids, cracks, fibres, etc.

In the paper the application of the micro-CT was used to obtained 3D images of the microstructure of the different cellulose fibre cement boards produced by extrusion pulping process. Main goals of the micro-CT analysis were focus on examination of a dispersion of the different origin fibres in the matrix.

Additionally, the evaluation of the microstructure, both cellulose fibres and fibre cement composites was performed using optical microscope in transparent light and scanning electron microscope.

2. Materials

Three sets of specimens made with three different fibre cement boards fabricated using extrusion process undergone the examination. The boards were reinforced by using both cellulose and polyvinyl alcohol (PVA) fibres to achieve the best mechanical performance. Polyvinyl alcohol is adopted from polyvinyl acetate which is readily hydrolysed by treating an alcoholic solution with aqueous acid or alkali [27]. At the beginning PVA is a white powder with specific gravity ranging from 1.2 to 1.3 g/cm^3, then this powder is formed and extruded to become PVA fibres which are commercially produced [28]. PVA fibres are characterized by high aspect ratio, high ultimate tensile strength, relatively high modulus of elasticity, good chemical compatibility with Portland cement, good affinity with water and no health risks [28,29]. Properties of PVA fibres are following: specific gravity 1.3 g/cm^3, diameter 0.014 mm, tensile strength 1500 MPa, Young's modulus 41.7 GPa.

Specimens – panels of the thickness of 10 mm – were made at the factory using the extrusion machines. This machines consists tree main parts: system which compress the mass at high pressure and forces it to extrusion die, which constitutes the shaped aperture that forms the boards, and last part – cutting device. The three steps: material preparation, board formation, and curing process were applied. Detailed description of the production process is covered by the manufacturer's secret know-how. The panels were cut in laboratory conditions using water-cooled saw. The small beams 100 mm × 20 mm × 10 mm were then subjected to further detailed tests.

Tested specimens are shown in Fig. 1 and comparison of tested panels are presented in Table 1.

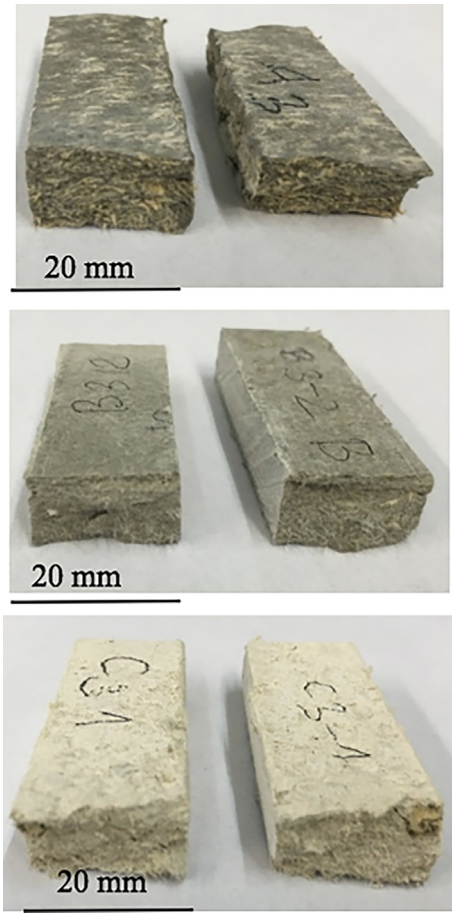

Fig. 1 – Tested specimens A, B and C.

The tested specimens were cut from the different fibre cement panels of 10 mm of thickness. Prior to the main research the panels were tested using the standard procedures to assess their performance. The material labelled 'A' was characterized by absorbability n_w (8–10%) and bending strength of panels 11–13 MPa. The concentration of fibres by weight in that material was equal 6% of good quality cellulose with length 2.5 mm. The material labelled 'B' was made using the same technology as 'A', but contained 6% of fibres by weight of recycled cellulose with length 1 mm and bending strength of panels 8.5–10 MPa. The material labelled 'C' was characterized by lower bending strength of 3–4 MPa and contained 4% of fibres by weight of good quality cellulose as a raw material with length 2.5 mm. Due to improper technology the cellulose matrix was damaged in specimen C. The orientation of fibres was non-uniform and several fibre agglomerates were present in the bulk material in the panels of type C what was possible to recognize by observing the fractured regions in that material.

The microphotographs of the applied fibres are shown in Fig. 2.

The homogeneity of the PVA fibres is clearly visible. The diameter of the separate fibre was 15–16 μm, and the length was about 6 mm. The cellulose fibres derived from the wastepaper [26] and from wood pulp (80% RH). All the cellulose fibres were characterized by heterogeneous form. It was

Table 1 – Characteristic of the tested three panels.

Characteristic of the tested panels	A	B	C
Type of panels	Fibre-cement, exterior	Fibre-cement, exterior	Fibre-cement, interior
Type of fibres	Cellulose from wood (pine)	Recycled cellulose from wastepaper	Cellulose from wood (pine)
Length of fibres [mm]	2.5	1.0	2.5
Content of fibres [%]	6	6	4
Form of application	Fibre pulp, 75% RH	Group of single fibres, dry	Fibre pulp, 100% RH
Thickness of panels [mm]	10	10	10
Average bending strength [MPa]	12.30	8.50	3.00
Average absorbability n_w [%]	9.63	9.38	19.54
Density [kg/m^3]	1700	1400	1200

Each panel contained the same amount of PVA fibre, ca. 1.0% with length 6.0 mm.

impossible to analyze only one single fibre - the cellulose fibres were grouped and shaped like nests. The fibres were flat in shape, without one specific dimension of diameter.

3. Test methods

The microstructural observations of the fibres were conducted in transmitted light. The image acquisition was performed using an Olympus BX51 microscope in plane-polarized light (PPL). Both, fibres and microstructure of the fibre cement panels were observed in scanning electron microscope SEM. The fresh fracture surface of the panel was analyzed by SEM-EDX. The piece of analyzed panel was mounted on a metal sample holder with the fracture surface of interest facing upwards. A strip of copper conductive tape was attached to each specimen to improve the conductivity of the whole specimen assembly. Finally, the specimens were examined using JEOL JSM-6380 LA Scanning Electron Microscope.

Nanotom 30 microtomograph made by General Electric operaying in the Institute of Materials and Machine Mechanics in Bratislava was used in the research. The following parameters were applied to perform the consecutive scans: lamp voltage – 115 kV, lamp current – 95 microamps, shot exposition time – 750 ms. The equipment was able to produce the following different data sets describing the specimen microstructure:

- digital specimen images representing cross-sections of investigated object derived in transverse or lengthwise direction to the mean axis of the cylindrical specimen,
- three-dimensional projections of specimens which are useful to present the high and low density regions of the entire specimen.

The space resolution of the reconstructed microstructure was 5 μm^3 per voxel. The result of micro-CT scanning was a set of tomograms (specimen cross-sections), performed every 5 μm of the specimen height. The set of tomograms consisted of 1200 cross-sections of 1200 $\times$ 1200 of bytes each. The total number of bytes related to consecutive voxels in such a dataset would be 1.7×10^9 bytes what may cause the further processing time-consuming. Therefore it was useful to take a certain subset from the entire dataset, preferably of cubic shape for further computations. The resulting subset is called a ROI (Region Of Interest) and is immune from the cracked areas situated in proximity of the specimen surface usually damaged by a drilling tool. In described research it was decided to process 3 ROIs of 930^3 (804,000,000) voxels each. This way the ROIs represented cubes of 4 mm $\times$ 4 mm $\times$ 4 mm were virtually extracted from investigated specimens.

4. Test results

The microstructure of the fresh split surface of the tested fibre cement panels is presented in Figs. 3–5. In all specimens the PVA fibres were oriented, they were arranged in one direction, parallel to the longer side of the panel. In the specimen A and C the nests of the cellulose fibres are visible, which may suggests improper mixing of the ingredients. The length of the fibres (shorter for B fibres) and form of application (group of single fibres for B) could influences the final microstructure of the panel. The microstructure of all specimens contained both types of fibres, PVA and cellulose fibres. The SEM microphotographs showed very good bond between cement matrix and cellulose fibres. The alkalinity of the cement paste is not corrosive for the material of the fibres, so the chemical bond exist and the adherence is ensured. In Fig. 5 the SEM-EDS analysis showed the chemical composition of the PVA fibre, cellulose fibres and cement matrix. It is visible that due to the strong bond between cellulose fibre and matrix, it was not possible to analyze the pure, single fibre. The content of calcium and traces of potassium and silica from cement matrix are present on the cellulose fibres.

5. Image processing procedures to assess the study of the microstructure of the fibre cement boards distribution

The obtained digitized datasets included the information about the material brightness in arbitrary units [a.u.] of all voxels of core volume, which is proportional to the local density of the material. After a study of obtained microtomograms it was found that the magnitudes of brightness were coded in following manner: the area of voids and fibres 0–50 [a.u.], the mortar area: 50–140 [a.u.], dense phases (unhydrated cement) and fine aggregate grains: 140–170 [a.u.]. The greyscale histograms of all voxels belonging to the investigated ROIs are presented in Fig. 6a. Fig. 6b depicts the results of investigation of four other specimens produced by Hatschek process and

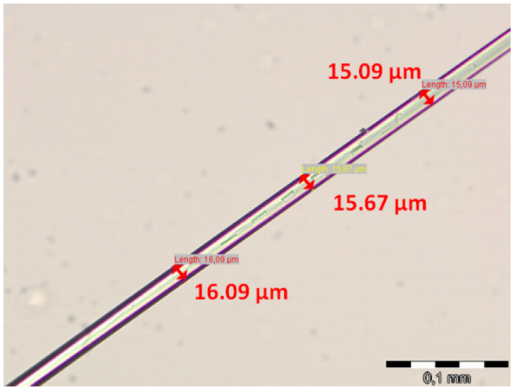

Single PVA fibre, observation in transmitted light, PPL, scale bar = 100 µm

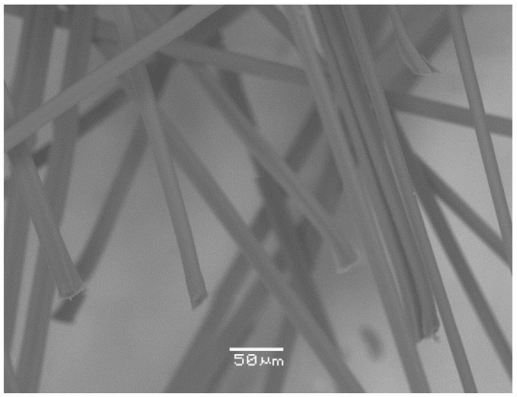

Single PVA fibres, SEM microphotograph, scale bar = 50 µm

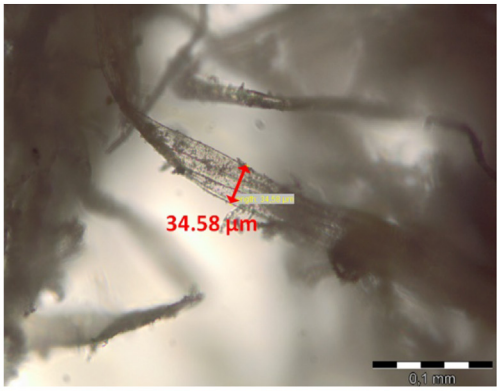

Single recycled cellulose fibre from the wastepaper, observation in transmitted light, PPL, scale bar = 100 µm

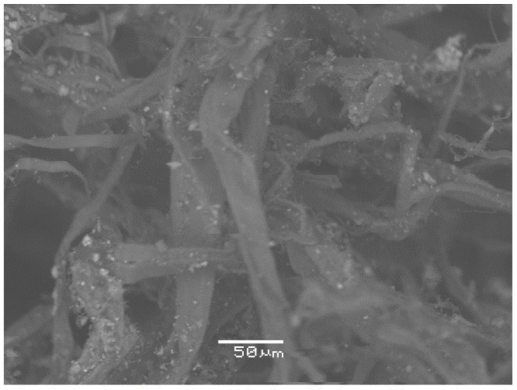

The bunch of the recycled cellulose fibres from the wastepaper, SEM microphotograph, scale bar = 50 µm

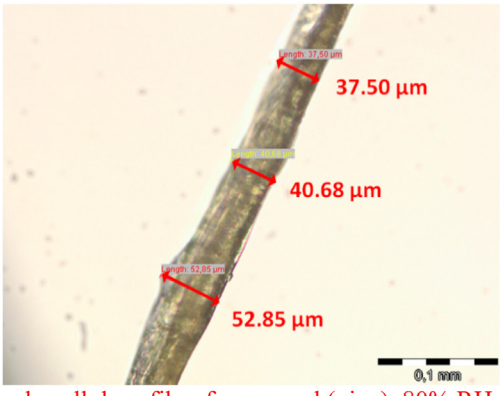

Single cellulose fibre from wood (pine), 80% RH, observation in transmitted light, PPL, scale bar = 100 µm

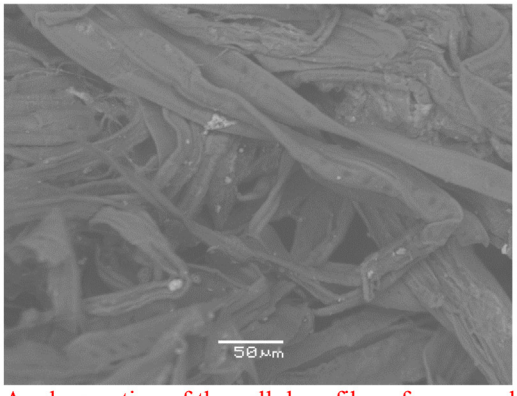

Agglomeration of the cellulose fibres from wood (pine), 80% RH, SEM microphotograph, scale bar = 50 µm

Fig. 2 – The microscopic observations of the applied fibres, left column: in transmitted light, plain polarized light (PPL), right column: in scanning electron microscope (SEM).

described in [21]. Labels denote the specimen code. The horizontal scale: voxel intensity [arb. units], the vertical scale: occurrence frequency [%].

Three dimensional view (ROIs) of investigated specimens A, B and C are depicted in Fig. 7. Black regions denote the low density regions of single fibres or fibres agglomerates.

Visualization of fibre system inside of the cubes cut off the A, B and C boards is presented in Figs. 8–10.

The graphs create on the basis of tomographic data clearly present the differences in fibre shapes in the two Figures mentioned above. The black coloured fibres presented in the images derived from specimen B are shorter and thinner than

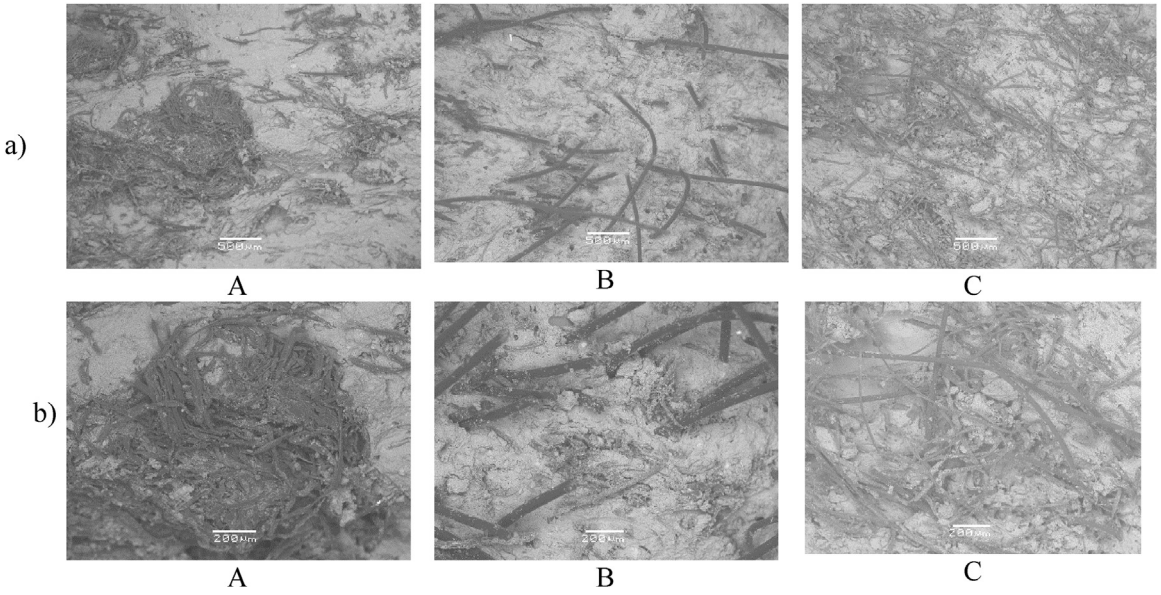

Fig. 3 – SEM microphotograph of the microstructure of three fibre cement panels, scale bar: (a) 500 μm, (b) 200 μm.

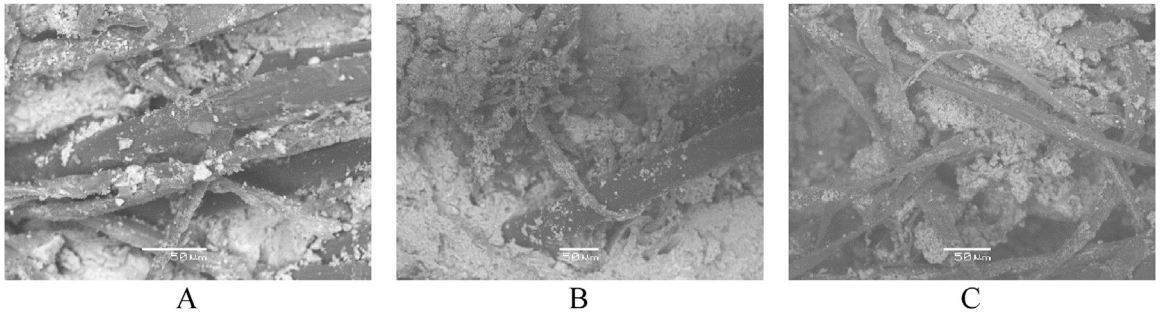

Fig. 4 – SEM microphotograph of the microstructure of three fibre cement panels, scale bar = 50 μm.

those depicted at the image related to the specimen A. There is also a large fibre agglomerate visible in the third image.

The other way to present the information included in the ROIs described above is to perform the brightness distribution of all voxels constituting the ROI ensembles. It was found that that the magnitudes of brightness of different regions existed in following manner: the area of voids and fibres 0–50 [arbitrary units, a.u.], fillers: 50–140 [a.u.], dense phases (unhydrated cement) and fine aggregate grains: 140–170 [a.u.]. The greyscale brightness distribution of all voxels belonging to the investigated ROIs are presented in Fig. 6a and b. One can mention that the presence of dense phases is resulted in a form of the peaks appearing at the right side of the distributions mentioned above. Analysing the mutual positioning of three curves in Fig. 6a one can mention that the curve representing the specimen C is shifted into left side due to presence of large fibre agglomerates, while the amount of fibres increases the amount of dark (i.e. low value) pixels. Otherwise the curve representing the specimen B3 is shifted to the right side from the centre due to the presence of smaller and shorter fibres, what results in the increase of bright pixels.

The example of visualization of fibre system inside of the cubes cut off the A, B and C boards is presented in Fig. 11. The digital data representing the local level of radiation absorption of scanned volume enables for different types of presentations.

The applied procedure to realize that latter task would compare the brightness of neighbouring voxels in order to find the low density regions mostly caused by the presence of fibres. That process is called a determining of the voxel *connectivity* and was described in [21]. The algorithm was earlier intended to simulate the diffusion of gases and liquids in the interconnected network immersed in bulk material. The authors have designed their own software to examine the voxel's interconnection in datasets resulted in micro-CT scanning. At the starting point of the action a certain number of 'walkers' was distributed randomly across the processed ROI. The 'walkers' occupied one voxel of space and could be understood as a marked point in the dataset representing the analyzed volume of the specimen. The walkers would migrate on neighbouring voxels obeying the information on voxels brightness (i.e. material density). The walkers would execute

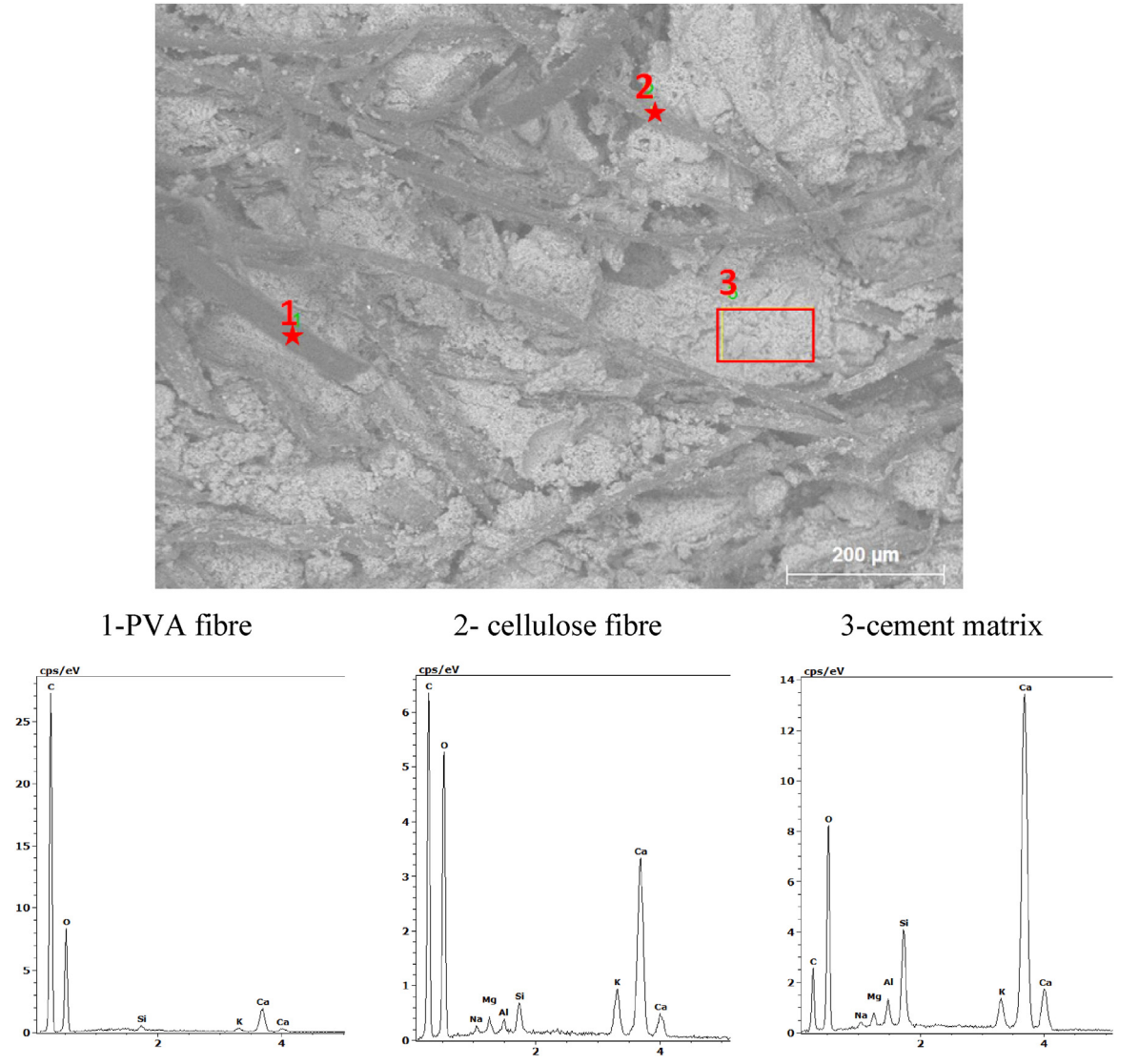

Fig. 5 – SEM microphotograph of the microstructure of the C fibre cement panels with microprobe analysis.

jumps in randomly chosen direction but the jumps could be performed if the neighbouring voxel belonged to a permitted light phase, otherwise the jumps were discarded. After refreshing the position of all walkers, one epoch of their action is completed by the algorithm. The number of epochs is measured by the dimensionless integer of time t. The primary output of the random walk procedure is the walker's mean-square displacement $\langle r(t)^2\rangle$ as a function of time (x_i, y_i, z_i are the coordinates of a current walker position and n is a number of operating walkers):

$$\langle r(t)^2\rangle = \frac{1}{n}\sum_{i=1}^{n}[(x_i(t)-(x_i(0))^2 + (y_i(t)-(y_i(0))^2 + (z_i(t)-(z_i(0))^2] \quad (1)$$

The key transport property called diffusion tortuosity τ of the porous medium is related to the time-derivative of $\langle r(\tau)^2\rangle$ and can be expressed as:

$$\tau = \frac{A}{d\langle r(t)^2\rangle/dt} \text{ as } t\to\infty \quad (2)$$

where A is the constant, which depends on implemented image lattice parameters and by some authors is assumed as 1.

The mean-square displacement $\langle r(t)^2\rangle$ in specimen A, B and in C equalled after 500,000 epochs respectively: 279, 4, 3160. The determined values of diffusion tortuosity τ, in turn, equalled: 52, 350, 16.5. One can mention that the cracked specimen is characterized by the parameters that significantly differ from the non-defected objects.

6. Conclusions

The presented microscopic and micro-CT observations of the fibres enabled for determination their shape and dimensions. The cellulose fibres were flat, without one specific dimension

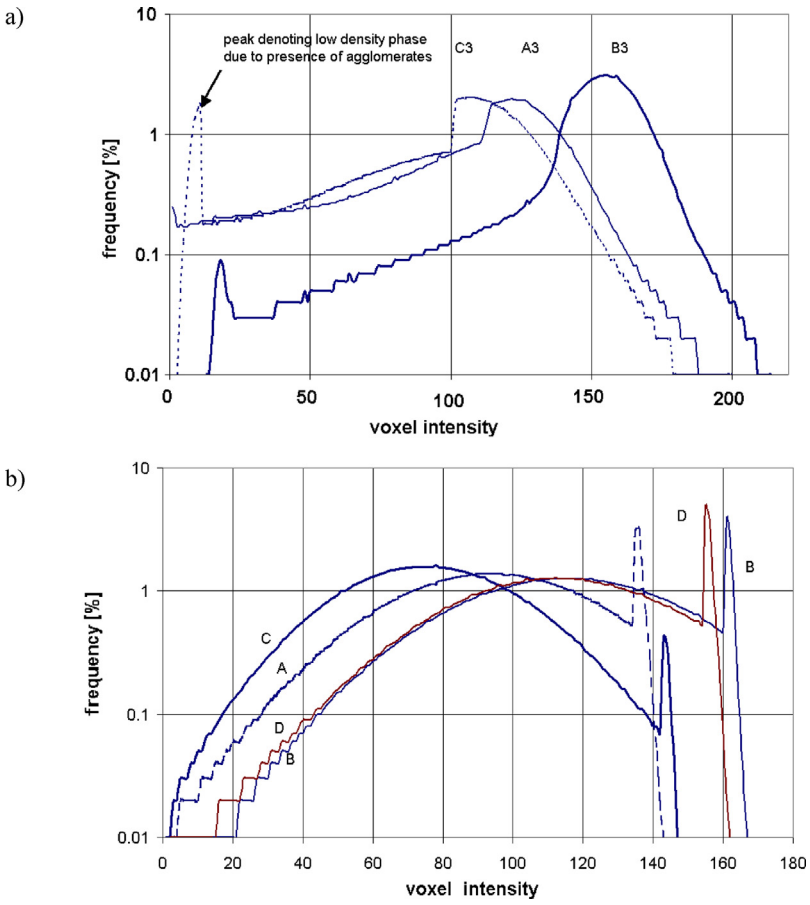

Fig. 6 – Greyscale value histograms for examined ROIs of the different fibre cement boards: (a) of three compositions described in the paper and produced by extrusion process, (b) of four specimens produced by Hatschek process and described in [21].

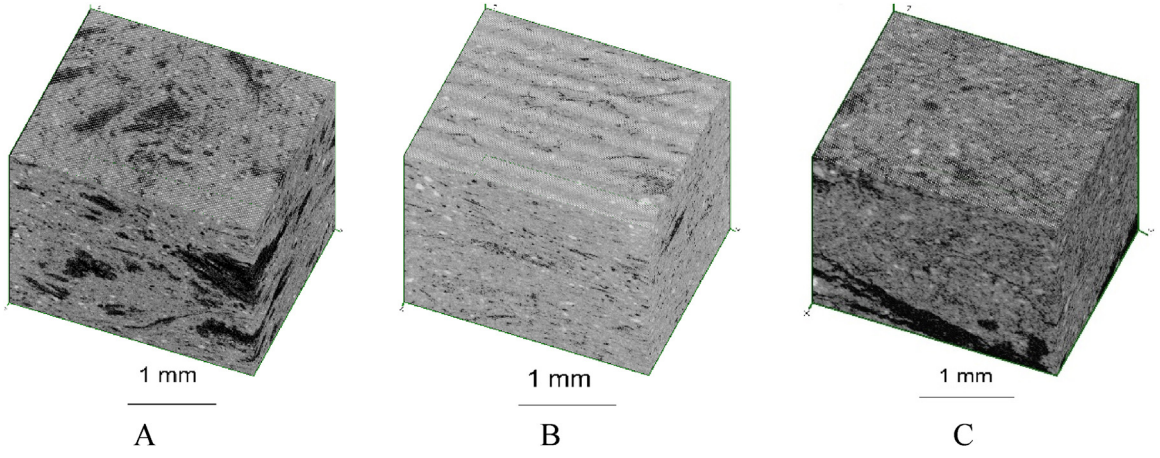

Fig. 7 – Three dimensional view of investigated specimens (left: A, centre: B and right: C). Black regions denote the low density regions of single fibre or fibre agglomerates.

of diameter in contrast to the PVA regular length and shape fibres. Moreover SEM microphotographs showed that cellulose fibres are useful as hybrid reinforcement, since a good bond between cement matrix and cellulose fibres was observed. In all tested specimens the PVA fibres were oriented, they were arranged in one direction, opposite to the cellulose fibres, which were grouped in a bunches. A dispersion of the different origin fibres in the matrix was observed.

The presented results of data obtained by investigation by micro-CT methods revealed that presented method can be

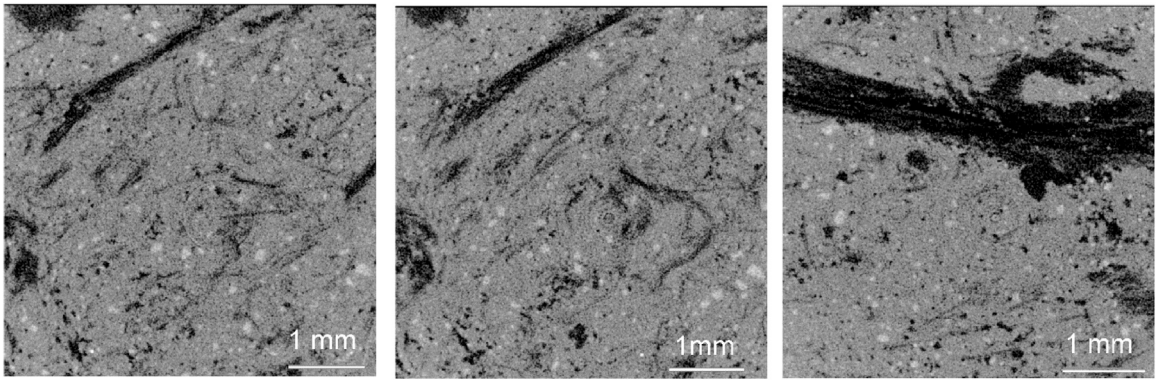

Fig. 8 – Examples of fibres recognized in board A. The fibres are of 200 μm diameter and ca. 3 mm of length (left and middle figure). A strand of fibres of cooperative width of 800 μm and cooperative length of 5 mm is seen at right figure.

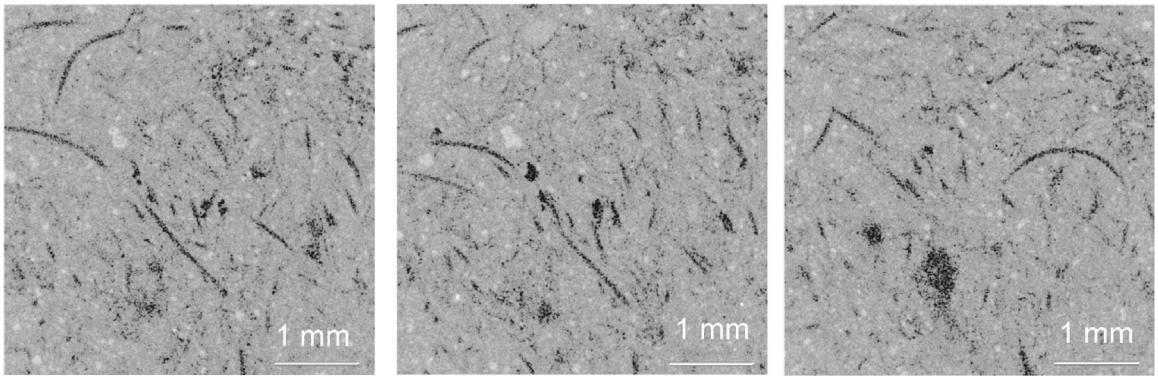

Fig. 9 – Examples of fibres recognized in board B. The fibres presented in figure are of ca. 40–50 μm of diameter and ca 1 mm length.

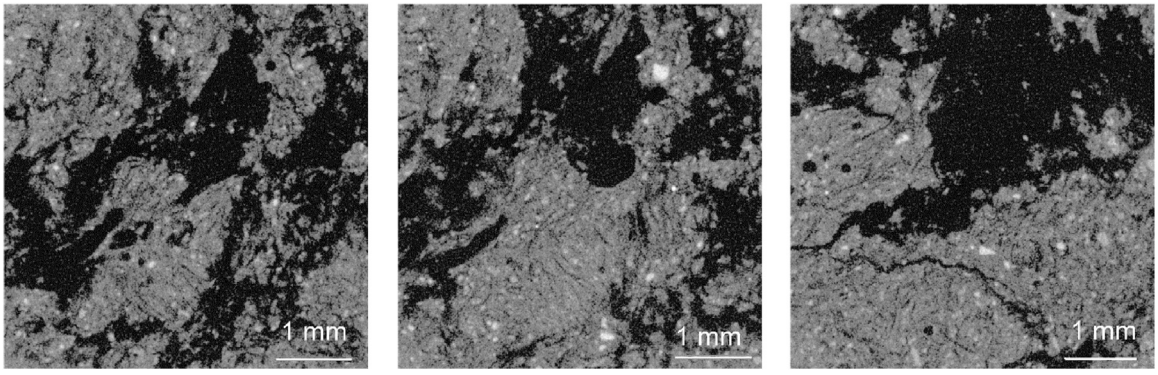

Fig. 10 – Examples of shapeless fibre agglomerates recognized in board C. The largest dimensions of these objects are in the range of 500–1000 μm.

used as a tool for analysis of fibre cement board microstructure, also a porosity of the matrix. The micro-CT method in comparison to others methods allow to present the microstructure of entire specimen volume in relatively fast and nondestructive mode. It should be notice that the resolution of detected details of microstructure strongly depends on the size of the investigated specimen.

The differences in material tightness of investigated specimens were established by applying measurements of water soaking ratio and bending strength. The results of the investigation using micro-CT method revealed the differences in the microstructure of the cellulose fibre cement composites due to variable fibre content or different kind of fibres. These differences in the microstructure were clearly visible on the images and could have been distinguished. Therefore, the described micro-CT method can be used as the supplementary tool for verifying the applied fabrication process an optimized percentage of fibres.

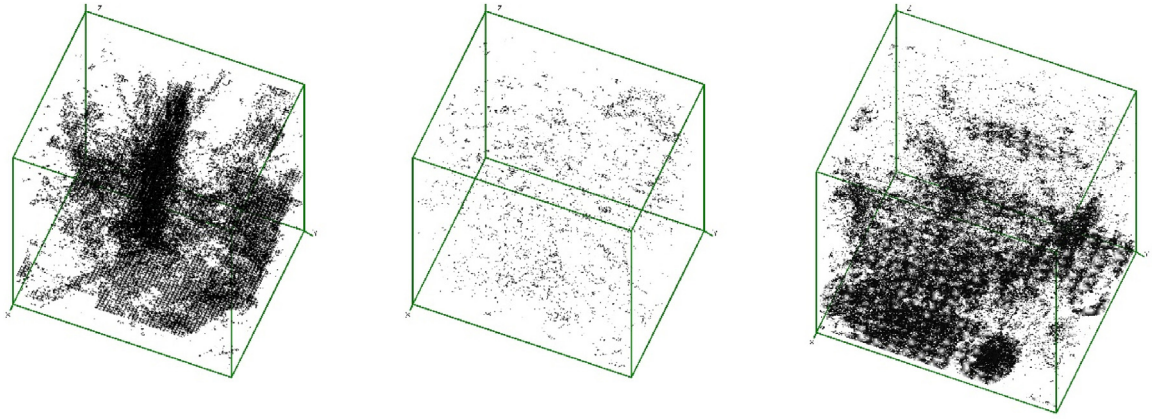

Fig. 11 – Visualization of fibre system inside of the cubes cut off the A, B and C boards.

Ethical statement

Authors state that the research was conducted according to ethical standards.

REFERENCES

[1] A.M. Brandt, Cement based composite materials with textile reinforcement, in: P. Hamelin, G. Verchery (Eds.), Proceedings of the International Symposium Composite Materials with Textile Reinforcement for Use in Building Construction and Related Applications, Edition Pluralis, Lyon, France, July 16–18, 1990 37–43.

[2] State-of-the-Art Report on Fibre Reinforced Concrete, ACI Committee 544, ACI 544.1-96, reapproved 2002, 2002, pp. 66.

[3] A.P. Fantilli, D. Jóźwiak-Niedźwiedzka, K. Gibas, J. Dulnik, The compatibility between wool fibres and cementitious mortars, 2nd International Conference on Bio-based Building Materials &1st Conference on ECOlogical valorisation of GRAnular and FIbrous materials, June 21st–23rd 2017, Clermont-Ferrand, France (in press).

[4] A. Akhavan, J. Catchmark, F. Rajabipour, Ductility enhancement of autoclaved cellulose fibre reinforced cement boards manufactured using a laboratory method simulating the Hatschek process, Constr. Build. Mater. 135 (2017) 251–259.

[5] M. Ardanuy, J. Claramunt, R.D. Toledo Filho, Cellulosic fibre reinforced cement-based composites: a review of recent research, Constr. Build. Mater. 79 (2015) 115–128. , http://dx.doi.org/10.1016/j.conbuildmat.2015.01.035.

[6] P.J. Kim, H.C. Wu, Z. Lin, V.C. Li, B. deLhoneux, S.A.S. Akers, Micromechanics-based durability study of cellulose cement in flexure, Cem. Concr. Res. 29 (1999) 201–208.

[7] EN 12467 – Cellulose Fibre Cement Flat Sheets. Product Specification and Test Methods, 2013.

[8] A.P.H. Westenbroek, Extrusion Pulping of Natural Fibres. Determination, Implementation and Verification of Constitutive Equations Required for Modelling, Wageningen, The Netherlands, 2000, . p. 150.

[9] L. Fernández-Carrasco, J. Claramunt, M. Ardanuy, Autoclaved cellulose fibre reinforced cement: effects of silica fume, Constr. Build. Mater. 66 (2014) 138–145.

[10] G.H.D. Tonoli, S.F. Santos, H. Savastano, S. Delvasto, R. Mejía de Gutiérrez, M.D.M. Lopez de Murphy, Effects of natural weathering on microstructure and mineral composition of cementitious roofing tiles reinforced with fique fibre, Cem. Concr. Compos. 33 (2011) 225–232.

[11] H. Savastano, P.G. Warden, R.S.P. Coutts, Microstructure and mechanical properties of waste fibre-cement composites, Cem. Concr. Compos. 27 (2005) 583–592.

[12] P. Soroushian, M. Elzafraney, A. Nossoni, H. Chowdhury, Evaluation of normal-weight and light-weight fillers in extruded cellulose fibre cement products, Cem. Concr. Compos. 28 (2006) 69–76.

[13] J. Hola, K. Schabowicz, State-of-the-art nondestructive methods for diagnostics testing of building structures – anticipated development trends, Arch. Civil Mech. Eng. 11 (2010) 5–11.

[14] J. Hoła, J. Bień, Ł. Sadowski, K. Schabowicz, Nondestructive and semi-destructive diagnostics of concrete structures in assessment of their durability, Bull. Polish Acad. Sci. Tech. Sci. 63 (1) (2015) 87–96.

[15] J. Hoła, Ł. Sadowski, K. Schabowicz, Nondestructive identification of delaminations in concrete floor toppings with acoustic methods, Autom. Constr. 20 (2011) 799–807.

[16] K. Schabowicz, J. Hoła, Nondestructive elastic-wave tests of foundation slab in office building, Mater. Trans. 53 (2012) 296–302.

[17] P. Berkowski, G. Dmochowski, J. Grosel, K. Schabowicz, Z. Wójcicki, Analysis of failure conditions for a dynamically loaded composite floor system of an industrial building, J. Civil Eng. Manage. 19 (2) (2013) 529–541.

[18] B. Goszczyńska, G. Świt, W. Trąmpczyński, A. Krampikowska, J. Tworzewska, P. Tworzewski, Experimental validation of concrete crack identification and location with acoustic emission method, Arch. Civil Mech. Eng. 12 (1) (2012) 23–28.

[19] Z.Z. Ranachowski, D.D. Jóźwiak-Niedźwiedzka, A.M. Brandt, T.T. Dębowski, Application of acoustic emission method to determine critical stress in fibre reinforced mortar beams, Arch. Acoust. 37 (3) (2012) 261–268.

[20] N. Neithalath, J. Weiss, J. Olek, Acoustic performance and damping behaviour of cellulose-cement composites, Cem. Concr. Compos. 26 (2004) 359–370.

[21] K. Schabowicz, Z. Ranachowski, D. Józwiak-Niedzwiedzka, L. Radzik, S. Kudela, T. Dvorak, Application of X-ray microtomography to quality assessment of fibre cement boards, Constr. Build. Mater. 110 (2016) 182–188. , http://dx.doi.org/10.1016/j.conbuildmat.2016.02.035.

[22] L.-P. Guo, A. Carpinteri, W. Sun, W.-C. Qin, Measurement and analysis of defects in high-performance concrete with three-dimensional micro-computer tomography, J. Southeast Univ. (Engl. Ed.) 25 (1) (2009) 83–88.

[23] V. Cnudde, J.P. Cnudde, C. Dupuis, P.J.S. Jacobs, X-ray micro-CT used for the localization of water repellents and consolidants inside natural building stones, Mater. Charact. 53 (November (2–4)) (2004) 259–271.
[24] J. Liu, C. Li, J. Liu, G. Cui, Z. Yang, Study on 3D spatial distribution of steel fibres in fibre reinforced cementitious composites through micro-CT technique, Constr. Build. Mater. 48 (November) (2013) 656–661.
[25] Q. Wang, X. Huang, W. Zhou, J. Li, Three-dimensional reconstruction and morphologic characteristics of porous metal fiber sintered sheet, Mater. Charact. 86 (December) (2013) 49–58.
[26] Waste Reduction Potential of Precast concrete Manufactured Offsite, Waste & Resources Action Programme, Mtech Consult Limited, Oxon, UK, 2010, http://www.wrap.org.uk/downloads/Pre-cast concrete-Full_case study.1fda4ebf.4510.pdf.
[27] F. Von Dorel, Polymeric Building Materials, vol. XVIII, Elsevier Applied Science, London/New York, 1989. p. 575.
[28] A. Noushini, B. Samali, K. Vessalas, Effect of polyvinyl alcohol (PVA) fibre on dynamic and material properties of fibre reinforced concrete, Constr. Build. Mater. 49 (2013) 374–383.
[29] T. Horikoshi, A. Ogawa, T. Saito, H. Hoshiro, G. Fischer, V. Li, Properties of polyvinyl alcohol fiber as reinforcing materials for cementitious composites, in: Proceedings of the International RILEM Workshop on High Performance Fiber Reinforced Cementitious Composites in Structural Applications, 2006, 145–153.